Low Methanol Permeable Sulfonated Poly(ether imide)/ Sulfonated Multiwalled Carbon Nanotube Membrane for Direct Methanol Fuel Cell

Yusun Heo, Sungjin Yun, Hyungu Im, Jooheon Kim

School of Chemical Engineering and Material Science, Chung-Ang University, Heukseok-Dong, Dongjak-Gu, Seoul 156-756, Korea

Received 16 September 2011; accepted 27 January 2012
DOI 10.1002/app.36881
Published online in Wiley Online Library (wileyonlinelibrary.com).

ABSTRACT: A novel organic/inorganic composite membrane synthesized with sulfonated multiwalled carbon nanotubes (s-MWNTs) and sulfonated polyetherimide (s-PEI) is prepared for use in a direct methanol fuel cell (DMFC). A solution casting method was used to prepare s-MWNT/s-PEI membranes (SPEI membranes) with various s-MWNT contents. This composite membrane showed not only low methanol crossover and water swelling but also enhanced mechanical properties. The IEC and proton conductivity of SPEI membranes were increased by incrementing their s-MWNT content. This is because the number of sulfonic acid groups (SO_3^-) increases as s-MWNTs are added. The water uptake of SPEI membranes increased as s-MWNT content was increased due to the hydrogen bonded interaction between sulfonic groups and carboxylic groups in s-MWNTs and water molecules. However, the water uptake of SPEI membranes is remarkably low, compared with Nafion membranes. The methanol permeability of the SPEI membranes (8.8×10^{-8} cm^2 s^{-1}) in this study was also lower than that of the Nafion membrane. Therefore, SPEI membranes were expected to have potential applications in DMFCs. © 2012 Wiley Periodicals, Inc. J Appl Polym Sci 000: 000–000, 2012

Key words: direct methanol fuel cell; multiwalled carbon nanotubes; polyetherimide; low methanol permeability

INTRODUCTION

Direct methanol fuel cells (DMFCs) have received attention as a promising power source in a wide range of applications, because they offer excellent advantages such as high efficiency, high power density, low noise, reduced pollution, simplicity, and reliability.[1,2] A proton exchange membrane (PEM) made from proton conductive material is the vital component of a DMFC; high proton conductivity and low methanol permeability are expected to be obtained. Up until now, perfluorosulfonic acid polymers such as Nafion® have been the reference membranes for DMFCs because of their excellent chemical resistance and mechanical stability as well as their high proton conductivity.[3,4] However, there are some specific limitations for Nafion®, including its very high cost, high methanol permeability, and loss of its preferable properties at a higher temperature.

Carbon nanotubes (CNTs) have attracted considerable interest due to their unique mechanical, thermal, and electrical properties. Because of these unique properties, CNTs were the preferred candidate to act as fillers in the development of nanotube-reinforced composites for both structural and functional applications.[5] These multiwalled carbon nanotube (MWNT) composites were expected to have multifunctional performance, including enhanced mechanical features for efficient load transfer, and high levels of electrical conductivity through a percolation network. However, CNTs are generally insoluble and formed bundles or bundle aggregates. Although CNT/polymer composites have great promise, their poor dispersion and the weak interface between the nanotubes and the polymer matrices are crucial problems to overcome for successful applications. The modification of the nanotubes is one of the most important approaches to overcome these problems.[6–11]

In recent years, many kinds of sulfonated aromatic polymers, such as poly(arylene ether)s, polyethersulfone (PES),[12] polyetherimide (PEI),[13,14] and polyvinylalcohol (PVA),[15] have been widely investigated as candidate PEM materials. These sulfonated aromatic polymers have good conductivity, thermal stability, and low cost.[16] However, they have a crucial water-swelling problem. Among these sulfonated aromatic polymers, aromatic imide thermoplastic polymers [such as polyimide and polyetherimide (PEI)] have been candidates for a variety of applications due to their excellent properties, such as high mechanical and chemical stability, solvent resistance, high heat

Correspondence to: J. Kim (jooheonkim@cau.ac.kr).
Contract grant sponsor: Chung-Ang University Freshman Academic Record Excellent Scholarship.

resistance, and good film-forming properties.[17,18] These polymers also serve as excellent matrices for multifunctional polymeric carbon nanocomposite materials. Polyetherimide (PEI), which has a similar imide group to polyimides, is also a high performance thermoplastic known for its high heat resistance and excellent mechanical properties even at elevated temperature due to its high glass transition temperature ($T_g \sim$ 216–220°C).[13,19–24] In previous work, PEI is used in DMFCs due to its excellent properties. Wen et al. reported on a membrane of blended sulfonated poly(ether imide) and poly(ether sulfone) for direct methanol fuel cells.[25] Additionally, Kumar et al. prepared a membrane of raw PEI blended with CNT. The CNT/PEI membrane showed better mechanical properties and higher thermal stability than a neat PEI membrane.[6] In this study, a novel s-MWNT/s-PEI membrane (SPEI membrane) was synthesized from sulfonated polyetherimide (s-PEI) and sulfonated MWNTs(s-MWNTs) for use in a DMFC. The effect of surface modification of MWNTs and PEI in the SPEI membrane is expected to result in good dispersion and enhanced membrane properties such as mechanical properties, water uptake, ion exchange capacity, proton conductivity, and methanol permeability.

Materials

The MWNTs (diameter, 20–30 nm; >99% purity) used in this study were supplied by Hanhwa Nano Tech (Seoul, Korea). Nitric acid (HNO_3, HPLC grade, Aldrich, Seoul), sulfuric acid (H_2SO_4, HPLC grade, Samchun Chemical, Pyungteak, Korea) and thionyl chloride ($SOCl_2$, HPLC grade, Samchun Chemical, Pyungteak, Korea) were used as received. Poly (ether imide) (PEI, Aldrich, Seoul), chlorosulfonic acid (Aldrich, Seoul), dichloroethane (DCE, Aldrich, Seoul), *N,N*-dimethylacetamide (DMAc, Aldrich, Seoul), methanol (MeOH, HPLC grade, Aldrich, Seoul), deionized water (DI water, HPLC grade, Aldrich, Seoul), sodium chloride (NaCl, Aldrich, Seoul) and phenolphthalein (PH indicator) were purchased from Sigma Chemical. Aminomethanesulfonic acid (TCI, Tokyo, Japan) was also used without further purification.

Synthesis of sulfonated PEI

As shown in Figure 1, the synthesis of s-PEI was carried out according to the following procedure.

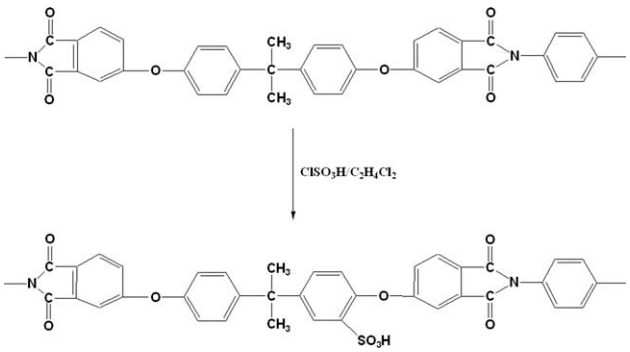

Figure 1 Sulfonation of PEI polymer.

The synthesis of s-PEI was carried out according to the following procedure. First, 5 g of PEI was dissolved in dichloroethane (30 mL) at 60°C for 2–3 h. The solution was stirred at 30°C for 1 h. Then the chlorosulfonic acid (1.5 mL) in DCE (27 mL) was slowly added drop-wise to the polymer solution under stirring. After 1 h, the product was dissolved in DMAc. The resulting sulfonated polymer was precipitated in isopropanol. The product was washed with isopropanol several times to remove excess acid and dried at room temperature. Then, the sample was dried in a vacuum at 60°C overnight.

Synthesis of the functionalized MWNTs

Figure 2 shows the scheme of functionalized MWNTs. The pristine MWNTs (0.2 g) were functionalized by heating in 40 mL of a mixture of concentrated H_2SO_4 (concentration: 98 vol %): HNO_3 (concentration: 70 vol %) (3 : 1 by vol %) under reflux. The concentration of raw MWNTs in the acid solution mixture was approximately 0.0025 wt %. The reactant was stirred at 50°C for 24 h and added to deionized water. The homogenous suspension was filtered through a 450 nm nylon membrane and washed several times. After the acid treatment, the resulting MWNT-COOH powder was dispersed in a $SOCl_2$ solution (250 mL) with stirring and sonication for 2 h and 12 h respectively, at 60°C. The suspension was vacuum-filtered through a 450 nm polytetrafluoroethylene (PTFE) membrane and dried for 12 h under vacuum at ambient temperature. Aminomethanesulfonic acid (2 g) was dissolved in 250 mL of deionized water followed by the addition of MWNT-COCl powder. This mixture was reacted under mechanical stirring at 80°C for 24 h. The resulting solution was

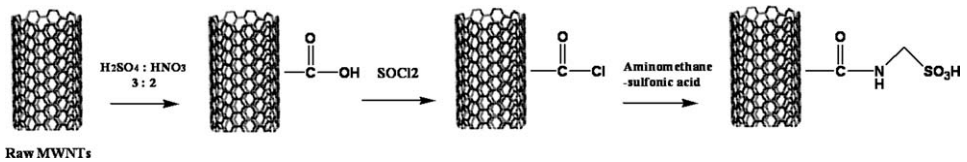

Figure 2 Sulfonation of MWNTs.

filtered through a 450 nm nylon membrane and dried at 100°C.

Preparation of s-MWNT/s-PEI (SPEI) composite membranes

The SPEI membrane was prepared using the solution casting method. The s-MWNTs were dispersed in DMAc and the weight ratios of the blends varied from 0 to 5%. The s-PEI (10 wt %) solution (based on DMAc) was blended with a suspended s-MWNT solution. The mixture of s-MWNT/s-PEI solution was stirred for 12 h and ultrasonicated for 10 min to obtain a homogeneous solution and cast onto Petri dishes at 150°C for 5–6 h. The fabricated s-MWNT/s-PEI (SPEI) membranes were peeled off the dishes. The thickness of the membrane was measured with a digital micrometer.

Characterization

Membrane characterization

The sulfonated polyetherimides were characterized by Fourier transform infrared (FTIR) spectroscopy [Bio-rad FTS-1465 (USA)] and ^{1}H-nulcear magnetic resonance (^{1}H-NMR) (Gemini 2000, Varian 300 MHz). The IR spectra were collected after 32 scans in the 4000–500 cm^{-1} region in ATR mode at a resolution of 4 cm^{-1}. The degree of sulfonation of the sulfonated polyetherimide was quantified by ^{1}H-NMR spectroscopy. Thermogravimetric analysis (TGA, TGA-2050, TA instruments) of the samples was carried out to examine the weight fraction of the functionalized MWNTs. The TGA measurements were carried out under a nitrogen atmosphere with a heating rate of 10°C min^{-1} from 30 to 780°C. The microstructural transformation of the s-MWNTs and SPEI nanocomposite membranes was analyzed by high resolution scanning electron microscopy (SEM, S-4300SE. Hitachi). The EDX measurements were performed with a Thermo NORAN System 7 EDX analyzer to measure the dispersion of sulfuric acid groups in the polymer. The tensile tests were carried out using an Instron 5565A universal testing machine at room temperature. The films, with various concentrations, were prepared into dog-bone specimens with dimensions of $3.82 \times 1.57 \times 1.24$ mm^3. The tensile strength of the films was measured with a gauge length of 20 mm and a crosshead speed of 1.3 mm min^{-1}.[26]

Water uptake

The SPEI membranes were dried at 80°C under vacuum for 12 h, and the weight of the dried membranes was measured. The membranes were immersed in deionized water at different temperatures (25, 60, and 80°C). After 24 h, the surface solution of the wetted membranes was removed with tissue paper. The wetted membranes were then reweighed. The uptake was calculated using the following equation[27]:

$$\text{Water uptake } (\%) = \frac{w_{\text{wet}} - w_{\text{dry}}}{w_{\text{dry}}} \times 100 \quad (1)$$

Ion-exchange capacity

The ion-exchange capacity (IEC) of the SPEI membranes was measured using the titration method. Dry SPEI membranes were immersed in 1 mol of NaCl solution for 24 h to replace all the H^+ with Na^+. The amount of H^+ protons released from the membranes was determined by titration, using a 0.01*M* NaOH solution with phenolphthalein as the PH indicator. The IEC value was obtained using the following equation[28]:

$$\text{IEC} = \frac{\text{consumed NaOH(mL)} \times \text{molatity of NaOH}}{\text{weight of dried membrane}} \times (\text{mequiv.g}^{-1}) \quad (2)$$

Proton conductivity

The proton conductivity of the SPEI membranes was measured by AC impedance spectroscopy (IM-6ex, Zahner) between 0.1 kHz and 1 MHz. Before the conductivity experiments, all samples were immersed in deionized water for at least 24 h at room temperature. These samples were sandwiched rapidly between the two Pt electrodes. The conductivity of all samples was measured using a two-point method at different temperatures (25, 60, and 80°C). The proton conductivity (σ) was calculated using the following equation[29]:

$$\sigma = \frac{h}{(R \bullet S)} \quad (3)$$

where h is the thickness of the conducting membranes, R (Ω) is the electro-resistance and S (m^2) is the surface area of the membranes.

Methanol permeability

The methanol permeability of the SPEI membranes was measured using a glass diffusion cell composed of two reservoirs, each with a capacity of 100 mL. Before each test, the membranes were prehydrated for at least 24 h. Each reservoir was separated by a prehydrated membrane. One part of the reservoirs was filled with a 10*M* MeOH solution, and deionized water was placed in the other part. Both

compartments were stirred continuously with a magnetic stirrer during the permeability experiment. The methanol permeability was found using the equation[29]:

$$C_B(t) = \frac{A}{V_B}\frac{DK}{L}C_A(t - t_0) \quad (4)$$

where C_A and C_B are the concentrations of MeOH in the donor and receptor reservoirs. A and L are the diffusion area and thickness of the membrane, respectively. The product of D and K is the methanol permeability ($cm^2\ s^{-1}$).

Determination of overall membrane characteristics

The required membrane characteristics for high performance of a DMFC are high proton conductivity and low methanol permeability. An evaluation of the membrane performance can be obtained using the following expression[30]:

$$\Phi = \frac{\sigma}{P} \quad (5)$$

where Φ is a parameter that evaluates the overall membrane performance in terms of the ratio of the ionic conductivity (σ) to the methanol permeability (P).

RESULTS AND CONCLUSION

ATR-FTIR spectra analysis

The results of ATR-FTIR analysis indicated the differences between pure PEI and sulfonated PEI spectra. Figure 3 shows the spectra of both (a) pure PEI and (b) PEI-SO_3H. The PEI and s-PEI spectra exhibit characteristic imide group absorptions at 1726 and 1778 cm^{-1} (imide carbonyl asymmetrical and symmetrical stretching), at 744 and 1357 cm^{-1} (C—N stretching and bending), and at 1238 cm^{-1} (aromatic ether, C—O—C).[6,27,28] Figure 3(b) shows the FTIR spectra of the s-PEI, in which a new peak appeared at $\sim$ 1684 cm^{-1}, which have shown typical absorbances for the sulfonic acid group (-SO_3H). The band at 1684 cm^{-1} could be explained as due to intermolecular hydrogen bonds between the hydrogen from the sulfonic (-SO_3H) and the carbonyl (C=O) groups.[20] Other bands due to S—O symmetrical vibration (O=S=O stretch) at 1240 cm^{-1} and O=S=O symmetric stretch at 1175 cm^{-1} were also present. Furthermore, the broad band in the s-PEI spectra around 3400–3450 cm^{-1} was assigned to O—H vibration associated with the interaction between sulfonic acid groups and water molecules.[18] This suggests that the sulfonic acid groups were successfully introduced into the PEI.

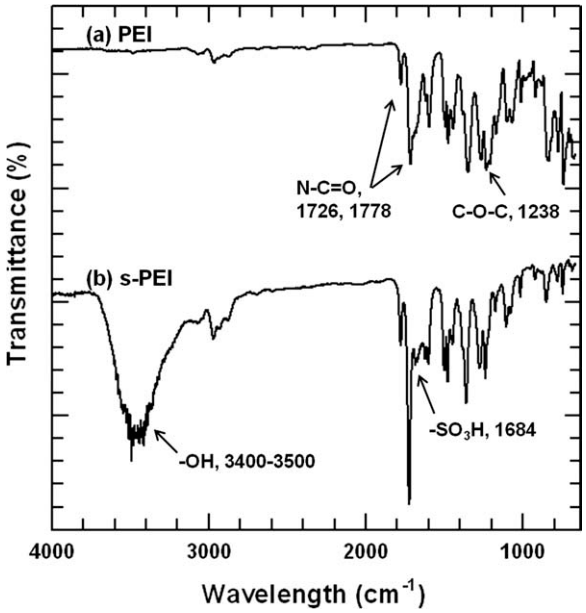

Figure 3 FTIR spectra of (a) pure PEI and (b) s-PEI.

^{1}H-NMR analysis

The sulfonation of PEI (s-PEI) is identified from ^{1}H-NMR spectroscopy. Figure 4 shows the ^{1}H-NMR spectra of (a) PEI and (b) s-PEI. In the PEI spectra, the signals attributed to the following aromatic protons: b proton (7.01–7.02 ppm), i proton (7.26 ppm), a proton (7.31–7.34 ppm), h proton (7.41 ppm), c proton (7.51 ppm), f and g protons (7.57 ppm), e proton (7.64 ppm), and d proton (7.89 ppm). Moreover, the spectra of s-PEI show the appearance of a singlet at 7.79 ppm corresponding to the protons adjacent to the sulfonic group. The introduction of the SO_3H group into the PEI results in a significant downfield shift from $\sim$ 7.10 to $\sim$ 7.99 ppm. The down field signals are attributed to the following protons of s-PEI: i′ proton (7.12 ppm), a′, b′, and h′ protons (7.25$\sim$ 7.45 ppm), f′ and g′ H (7.65 ppm) and d′ proton (7.99 ppm).

The degree of sulfonation (DS) was measured by ^{1}H-NMR. In the chemical structure of s-PEI, there are 16 aromatic protons in the sulfonated repeat units compared with 18 aromatic protons in the non-sulfonated repeat units of pure PEI. The peak at 7.79 ppm, which is attributed to the proton adjacent to the sulfonic group, is well distinguished from all other peaks. The degree of sulfonation is given by:

$$R = \frac{A_e}{A}, \quad DS = \frac{18R}{1 + 2R} \quad (6)$$

Here, R is defined as the ratio of the area under the peak at 7.79 ppm, A_e, to the sum of the area under the peaks corresponding to all the other aromatic protons, A.[24,31,32] The degree of sulfonation of s-PEI is 0.577.

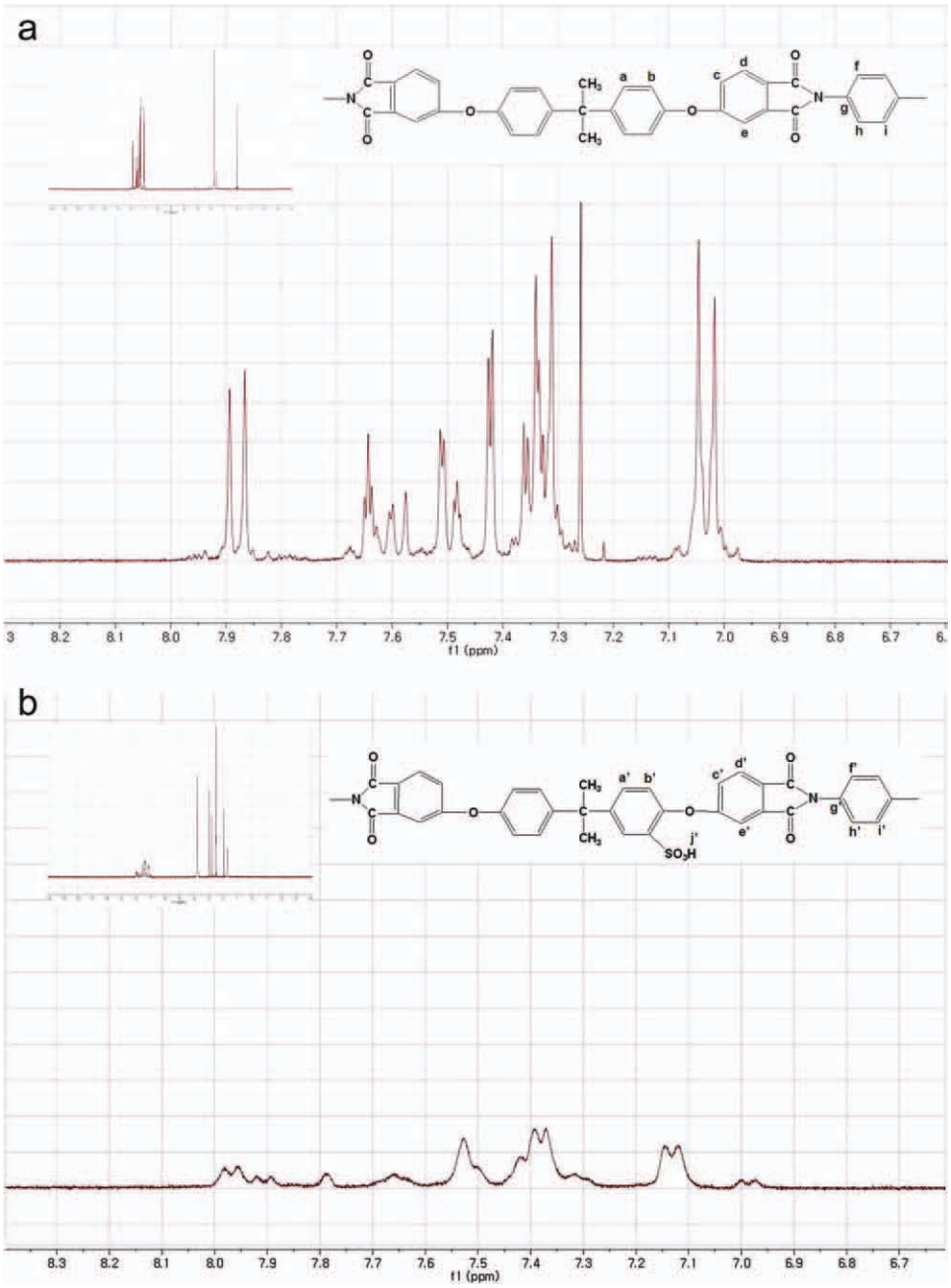

Figure 4 ^{1}H-NMR spectra of (a) pure PEI and (b) s-PEI. [Color figure can be viewed in the online issue, which is available at wileyonlinelibrary.com.]

Raman spectroscopy

Raman spectroscopy is used to characterize the structural changes of pure MWNTs and fuctionalized MWNTs. In Raman spectra, we observe the peak of the G-band at 1585 cm^{-1} which is assigned to the stretching of the C—C bond and the peak of the D-band at 1359 cm^{-1} originating from defects and disorder in the graphitic structure. As shown in Figure 5, the D-band intensity was increased in functionalized MWNTs compared with pure MWNTs. This indicates that the number of defects in the MWNTs is increased, which is attributed to the functionalization of the carboxyl groups and sulfonic groups in the MWNTs. In addition, the D′-band at 1620 cm^{-1}, which is affected by disorder in the nanotubes, also presents at different intensities for pure and functionalized MWNTs. Because the D′-band is not observed for pure MWNTs but is clearly detectable after functionalization, the D′- band in functionalized MWNTs is also evidence of an increase in the number of defects (the functionalized sites in MWNTs) in s-MWNTs. The I_D/I_G peak intensity ratios of functionalized MWNTs exceeded those of pure MWNTs. These results

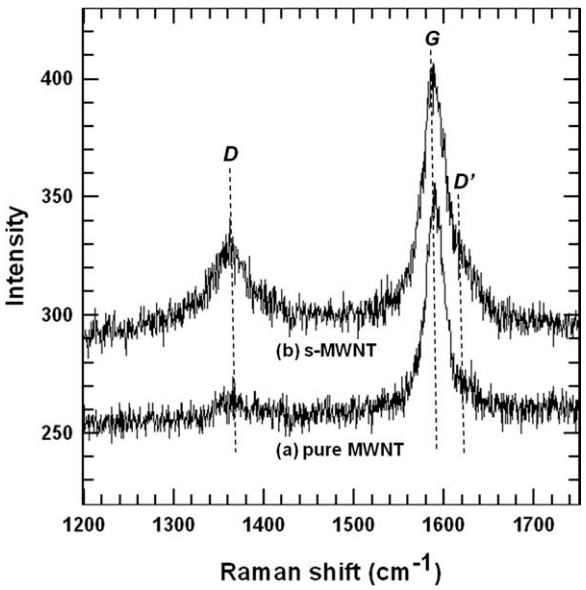

Figure 5 Raman spectra of (a) pure MWNTs and (b) s-MWNTs.

provide direct evidence of the modification of MWNTs.

EDX and SEM analysis

EDX confirmed the existence of sulfonic acid groups on the surface of the s-MWNTs and sulfonic groups ($-SO_3$) in the polymer. The EDX spectrum of s-MWNTs [Fig. 6(b)] was examined and found to contain an additional sulfur peak, whereas the spectrum of the pristine MWNTs [Fig. 6(a)] showed only carbon and oxygen peaks. The results confirmed the presence of sulfonic acid groups on the surface of MWNTs. Moreover, the oxygen peak of s-MWNT is approximately two times bigger than that of pure MWNT, which is attributed to the oxygen atoms of sulfonic groups and remaining carboxyl groups. Also, the nitrogen peak in the s-MWNT spectrum, which is attributed to aminomethanesulfonic acid, is detected as a very small peak. This is because EDX is not good at detecting nitrogen atoms. Figure 7(a) (s-PEI) presents the EDX spectrum of the s-PEI matrix. It indicates the presence of sulfur in the polymer. The Pt peaks correspond to the Pt coating. Sulfur mapping [Fig. 7(b)] confirmed that the sulfonic acid content was well distributed in the s-PEI matrix.

Field emission scanning electron microscopy (FE SEM) was used to confirm the dispersity of MWNT/s-PEI membranes [Fig. 8(a)] and 5 wt % s-MWNT/s-PEI membranes [Fig. 8(b)]. As shown in Figure 8(a), the pure MWNTs were ununiformly distributed throughout the entire surface and aggregated. This is because of the large surface energy of the tubes and the high viscosity of PEI. Another possible explanation may be the increase in viscosity, which could not support the uniform dispersion of the tubes and resulted in the formation of agglomerates.[5] In contrast, Figure 8(b) (s-MWNTs) shows well-separated nanotubes dispersed throughout the entire surface without any agglomerates. The reasons for these results can be subdivided into two factors. First, the functionalized MWNTs (s-MWNTs) and functionalized polymers (s-PEI) formed a strong interaction. This suggests that the interfacial interaction of MWNTs and PEI was increased by the introduction of sulfonic acid groups into each material. Secondly, the chemical reaction between the remaining COOH groups on the MWNT and the polar group (CONCO) along the polymer chain increases the interfacial adhesion between the polymer/matrix and the nanotubes. That is, -O- groups on PEI chains may form hydrogen bonds with –COOH groups on MWNTs.[6] This chemical reaction between the COOH-MWNT and PEI is very compact and strong, as compared with the physical interaction (π-stacking or noncovalent interaction) between the untreated MWNT and PEI.

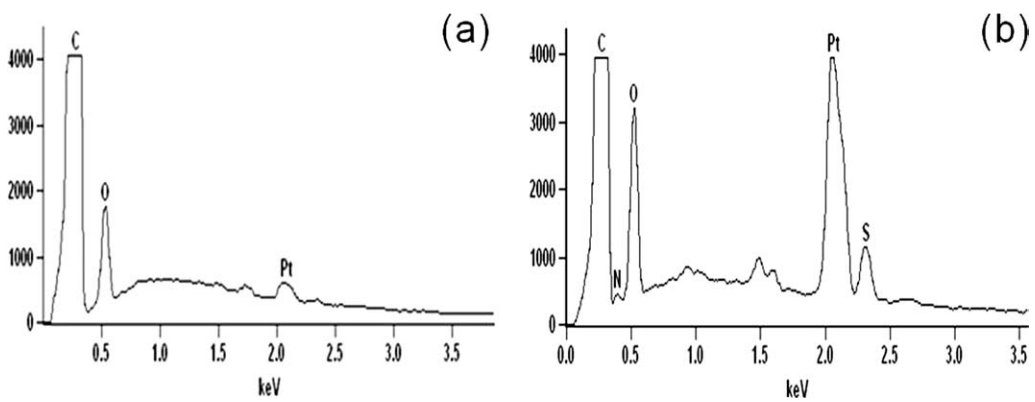

Figure 6 EDX spectra of (a) pristine MWNTs and (b) s-MWNTs.

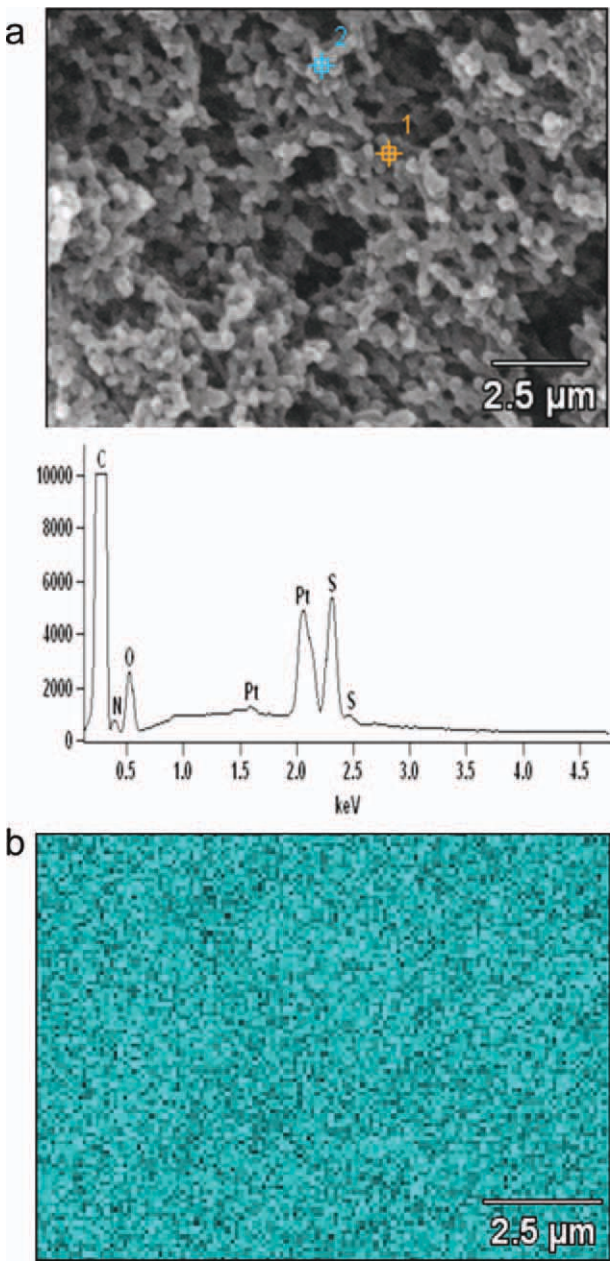

Figure 7 (a) EDX spectrum of s-PEI and (b) sulfur mapping. [Color figure can be viewed in the online issue, which is available at wileyonlinelibrary.com.]

Thermal analysis of SPEI membranes

Thermal stability is a crucial property for durability during fuel cell operation at high temperature. TGA was performed on SPEI membranes with different s-MWNT contents. The s-PEI/s-MWNT membranes show overall higher thermal stability compared with the pure s-PEI. This was attributed to interaction between the sulfonic groups of s-MWNTs and those of s-PEI. That is, the chain entanglement between the sulfonic groups on the nanotube surface and polymer matrix leads to high interfacial adhesion. There is also interfacial bonding between carboxylic groups on the MWNTs and polar groups (CONCO) in the polymer. Thirdly, CNTs have good barrier action. Increased thermal resistance is attributed to the carbon nanotube barrier effect slowing down the products' volatilization. The confinement of polymer chains onto the surface of well-dispersed carbon nanotubes restricted the segmental motion and suppressed chain transfer reactions.[6] In N_2 atmosphere, thermal degradation of s-PEI/s-MWNTs appeared in two steps. As shown in Figure 9, the first step (180–200°C) most likely originated from the presence of labile methyl groups present in PEI. The second thermal degradation, at a temperature of approximately 350°C, is believed to be associated with the sulfonic acid group. Finally, weight loss appeared at 530°C, which might be near the decomposition temperature of the PEI chain.[33,34]

Tensile testing

The addition of functionalized MWNTs as the filler was expected to enhance the mechanical properties of the membrane. Table I shows the tensile strength data for s-PEI and SPEI membranes with different s-MWNT loadings (The data in Table I are average values). The tensile strength of the SPEI membranes ranged from 46.74 to 58.03 MPa and the elongation at breaking ranged from 9.15 to 11.13%. Because the s-MWNTs in the SPEI membranes tend to aggregate when the s-MWNT content is increased, the SPEI membrane becomes brittle. The decreased tensile strength value at 5 wt % loading SPEI membrane is due to the brittleness of the SPEI membrane. However, the SPEI membrane becomes stiffer as s-MWNT content is increased, which is represented by the increasing of Young's modulus. The values of these mechanical properties are higher than those of raw MWNT/PEI membranes.[35] These enhanced mechanical properties of SPEI membranes as compared with raw MWNT/PEI membranes were effected by strong interfacial interactions between functionalized nanotubes (s-MWNTs) and the functionalized PEI matrix (s-PEI). Another factor of the strong interaction is the increase in sites (the remaining –COOH groups of MWNTs) that can react with polar groups (-CONCO-) in the PEI matrix. That is, the improved mechanical strength data is attributed to increased adhesion between filler and matrix and homogeneous dispersion of modified MWNTs in the s-PEI matrix. As a result, the SPEI membrane appeared to have excellent mechanical properties due to the functionalized MWNT reinforced polyetherimide systems. The tensile strength value of the SPEI membrane was higher than those of Nafion 117 (10 MPa) and Nafion 112 (22.6 MPa).[24,36] This result indicated that the SPEI membrane is suitable for use in a DMFC.

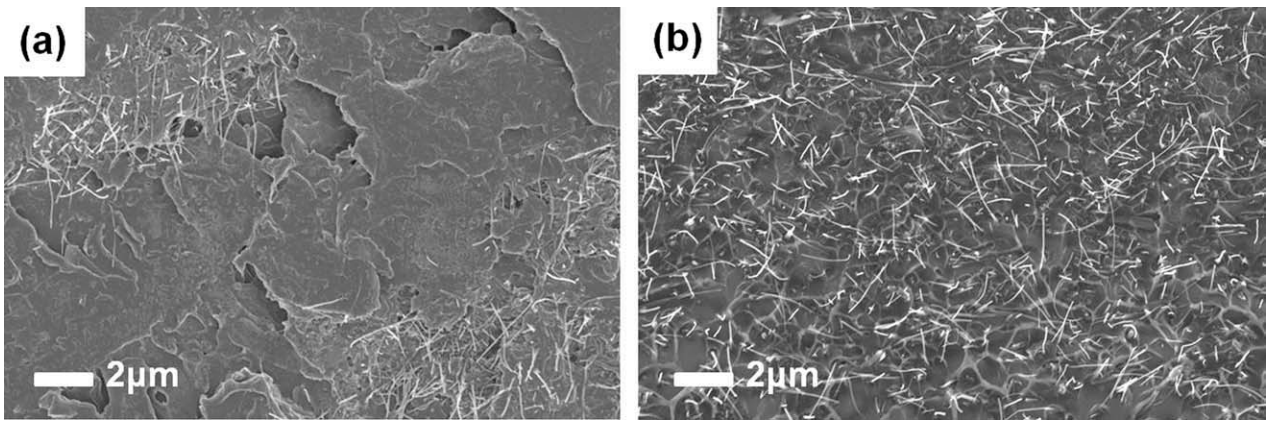

Figure 8 SEM images of (a) pure MWNTs/PEI membranes and (b) SPEI membranes.

Water uptake

Water uptake in proton exchange membranes plays a crucial role in proton conductivity. The water within the membrane provides a carrier for protons; that is, protons can transport along hydrogen-bonded ionic channels, and the proton conductivity is very dependent on the connectivity of the hydrated domains. However, when the water uptake exceeds its limit in the membranes, it has an unfavorable influence on the mechanical properties and dimensional stability.[13,36,37] Therefore, it is important to mediate the water uptake amount in a DMFC. Figure 10 shows the water uptake of SPEI membranes at 25, 60, and 80°C. The water uptake of SPEI membranes increased with increasing s-MWNT content. These results indicate the effect of the increasing number of sulfonic groups (SO_3^-) in s-MWNTs which formed hydrogen bonds with water molecules. Another reason is that the carbonyl groups of s-MWNTs also formed hydrogen bonds with water molecules. Figure 10 also shows the temperature dependence of water uptake. It confirms that the water uptake of SPEI membranes increased with increasing temperature, which was due to the greater mobility of polymer chains at higher temperature.[36] The water uptake value of the SPEI membrane is considerably lower than that of the Nafion 117 (33 wt %).[28] This results is attributed to the difference in chemical structure between the SPEI membrane and Nafion. The main chain of s-PEI is almost organized, with highly rigid aromatic groups, whereas that of the Nafion membrane is well composed of flexible linear fluorinated chains. In addition, long-grafted ionic groups in the Nafion membrane enhance the plasticity of the polymer and water absorption increases, in contrast to SPEI membranes where the

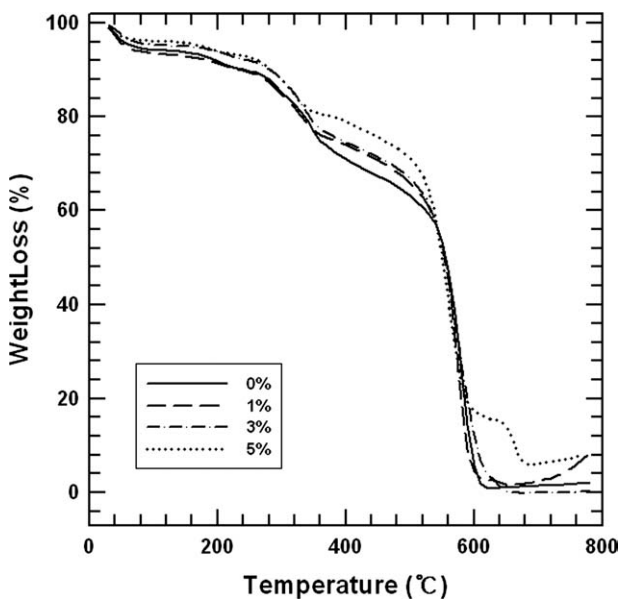

Figure 9 The thermal analysis of SPEI membranes (TGA).

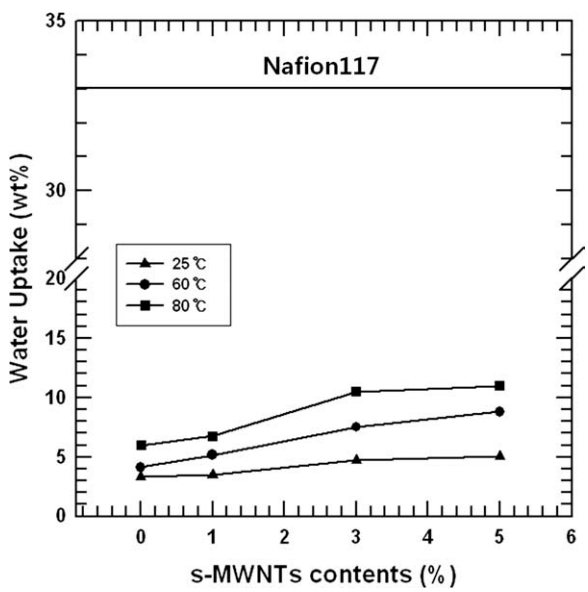

Figure 10 Water uptake of SPEI membranes at 25, 60, and 80°C.

TABLE I
The Mechanical Properties of SPEI Membranes

SPEI membrane	Tensile strength (MPa)	Young's modulus (N mm^1)	Elongation at break (%)
Pure PEI	60.5	33.6	13.7
0 wt % s-MWNT/s-PEI	56.1	29.7	9.8
1 wt % s-MWNT/s-PEI	57.3	34.3	10.4
3 wt % s-MWNT/s-PEI	58.4	38.8	11.2
5 wt % s-MWNT/s-PEI	51.2	48.6	9.3

TABLE II
Water Uptake, Proton Conductivity, and Methanol Permeability Data at 80 °C

s-MWNTs contents (wt %)	Water uptake (%)	Proton conductivity (mS cm^{-1})	Methanol permeability ($\times 10^{-8}$ cm^2 s^{-1})
0	5.99	0.02	0.04
1	6.75	0.29	0.19
3	10.51	2.32	0.88
5	11.00	3.98	1.17

sulfonic acid groups are directly attached to rigid polymer chains. That is, the structure of the SPEI membrane is too rigid to be swollen when the water molecules get through the polymer, while the flexible chain of the Nafion membrane is freely expanded to form and aggregate ionic water clusters.[28,36,38] As a result, the SPEI membrane has a lower absorption ratio of water than that of Nafion. Therefore, the SPEI membrane was expected to improve upon the high water uptake of the Nafion membrane.

Ion exchange capacity

The ionic exchange capacity depends on the molar ratio of the sulfonic group in the polymer chain and the molar weight of the repeated unit.[36,39] It plays a crucial role in proton conductivity in DMFC applications. The titrated IEC values were used to estimate to the contents of fixed SO_3^- sites in the membranes. Figure 11 shows the IEC values of SPEI membranes at room temperature. As the s-MWNT content was increased, the IEC values of the SPEI membranes increased from 0.66 up to 0.98 mequiv g^{-1}. This result was obtained because the s-MWNTs and s-PEI have the sulfonic acid group (SO_3^-) as the fixed charge site. The increased s-MWNT content enhances the suitable sulfonating sites, which corresponds to the increase in charge carriers in the membranes.

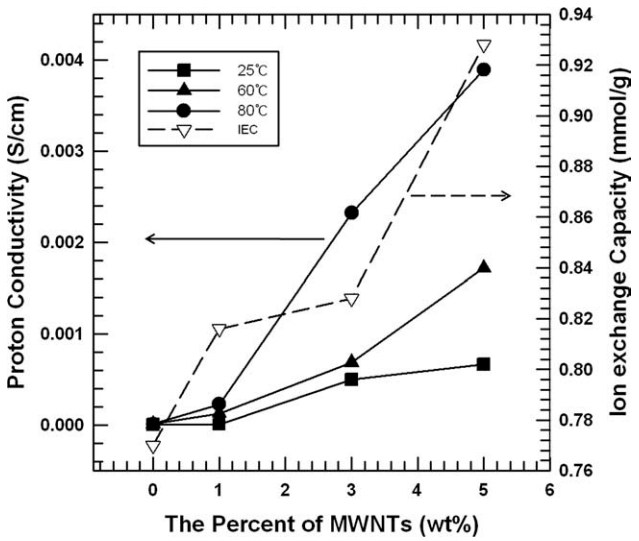

Figure 11 Ion exchange capacity of SPEI membranes at room temperature and proton conductivity of SPEI membranes at 25, 60, and 80°C.

Proton conductivity

Proton conductivity is the most vital requirement to enable membranes to be applicable in direct methanol fuel cells. As shown in Figure 11, the proton conductivity of the SPEI membrane was measured at temperatures ranging from 25 to 80°C. The proton conductivity of the SPEI membrane reached a value of 0.004 S cm^{-1}. As the s-MWNT content was incremented, the proton conductivity of SPEI membranes increased. This is because the s-MWNTs that were used as a filler in the matrix contain sulfonic groups. The sulfonic groups raise the conductivity of the SPEI membrane not only by increasing the number of protonated sites (SO_3H), but also through the formation of water mediated pathways for protons. In Table II, it is indicated that the proton conductivity increased with increasing water uptake. This is because the proton conductivity of a polyelectrolyte membrane depends on its water content. There are two types of proton conduction mechanisms: the vehicular mechanism and the Grotthus mechanism. Both of these mechanisms are strongly related to water uptake. In the vehicular mechanism, water molecules act as vehicles by carrying along protons that are attached to them in such forms as H_3O^+, $H_5O_2^+$, $H_9O_4^+$ while diffusing through the aqueous media. Meanwhile, the Grotthus mechanism involves stationary water molecules, with protons hopping from one water molecule to another to be transported along hydrogen bonded ionic channels.[40,41] That is, the more water that exists in the membrane, the more hydrated species are generated, thus, the more protons are transported.

In this study, the proton conductivity of s-PEI membrane is very low due to the structure of the s-PEI backbone chain, which is too rigid to be swollen, and its dependency on water content. However, the proton conductivity of SPEI membranes achieves

a maximum value of (3.98×10^{-3}S cm^{-1}) as the s-MWNT content is increased. As mentioned earlier, this is because of the increased number of s-MWNTs, which contains many sulfonic groups. That is, sulfonic groups provide more charge carriers for the ionic conduction. These effects of sulfonic acid ions in the SPEI membrane lead to better performance in terms of proton conductivity. It is found that the proton conductivity of SPEI membranes is high compared to their low water absorption.

Methanol permeability

Methanol permeability is also important for DMFC applications. The membrane of the DMFC can use high methanol concentrations at low methanol permeability. As a result, a low methanol permeability results in an excellent effective energy density in the DMFC system.[13] Table II shows the methanol permeability of the SPEI membranes. The values of methanol permeability in SPEI membranes increased from 4.91×10^{-10} to 1.17×10^{-8} cm^2 s^{-1} with incrementation of s-MWNT content. These values were remarkably lower than that of Nafion 117 (2.91×10^{-6} cm^2 s^{-1}).[36] This result is due to the differences between the microstructures of these two polymers. The Nafion membrane, due to the extremely high hydrophobicity of the perfluorinated backbone and high hydrophilicity of the sulfonic acid groups, leads easily to hydrophobic/hydrophilic separation. The sulfonic acid groups aggregate to form hydrophilic domains. The well-connected hydrophilic domains function as a substance transport channel. Not only protons and water but also some smaller polar molecules such as methanol can get through these channels. This phenomenon leads to methanol permeability. However, the structure of SPEI membranes is such that the backbone of sulfonated polyetherimide is rigid and less hydrophobic, while the sulfonic acid group is less acidic and therefore less hydrophilic. As a result, the hydrophobic/hydrophilic domains of SPEI membranes are less separated and the methanol permeability of the SPEI membrane is lower than that of the Nafion membrane.[1,2,42]

Overall membrane characteristics

Membranes intended for practical usage as PEMs in DMFCs are required to possess high proton conductivity and low methanol permeability.[43] The selectivity, which is defined as the ratio of proton conductivity to methanol permeability, is the factor for evaluating membrane performance in terms of both proton conductivity and methanol permeability. The selectivity factor is usually used as an indicator for the applicability of membranes by comparing its value with those of commercial materials. A higher selectivity value implies a better applicability in DMFCs. Figure 12 shows the selectivities of the Nafion, s-PEI, and SPEI membranes. The selectivity of the SPEI membranes was improved with the introduction of s-MWNTs and showed better performance than Nafion. These results were attributed to low methanol permeability compared with increasing proton conductivity. The maximum selectivity appears at 5 wt % of s-MWNT loading. This selectivity value of the SPEI membrane is approximately five times that of Nafion. Therefore, SPEI membranes are definitely promising materials for DMFC applications.

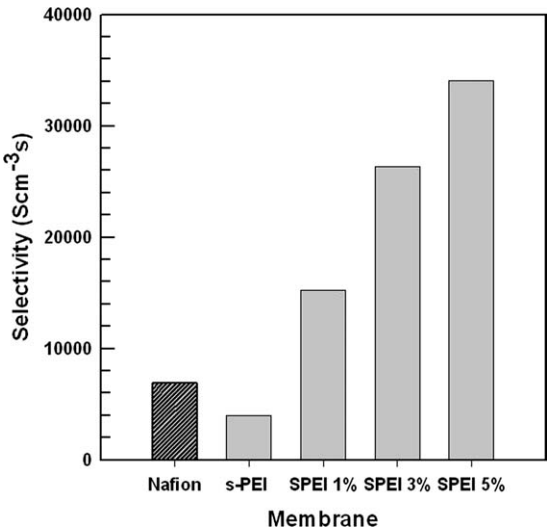

Figure 12 The selectivity (ratio of proton conductivity to methanol permeability) for Nafion, s-PEI, and SPEI composite membranes.

CONCLUSIONS

The composite membranes of sulfonated MWNTs (s-MWNTs)/sulfonated polyetherimide (s-PEI) with various s-MWNT contents were prepared using a solution casting method. The surface modification of MWNTs and PEI induces not only an increase in the number of sulfonic groups (SO_3H) in the SPEI membranes, but also improved adhesion between s-MWNTs and the polymer. The large interaction forces between s-MWNTs and s-PEI were formed by interaction effects of sulfonic acid groups in s-MWNTs and the polymer. Another interaction effect is the chemical reaction between the remaining COOH groups on the MWNTs and polar groups (CONCO) in the polymer. The homogeneous dispersion of s-MWNTs in the s-PEI matrix was attributed to these interaction forces. In the water uptake experiment, SPEI membranes absorbed three times less water than Nafion117, even for a similar IEC, due to the rigid structure of the main chain (s-PEI polymer). The SPEI membranes showed high

mechanical properties due to strong adhesion and low water swelling. The lower methanol permeability (1.71×10^{-8} cm^2 s^{-1}) and higher selectivity of SPEI membranes compared with Nafion was shown. These results indicated that the newly developed SPEI membranes are promising materials for DMFC applications.

References

1. Shang, Y.; Xie, X.; Jin, H.; Guo, J.; Wang, Y.; Feng, S.; Wang, S.; Xu, J. Eur Polym J 2006, 42, 2987.
2. Li, L.; Zhang, J.; Wang, Y. J Membr Sci 2003, 226, 159.
3. Yang, T. Int J Hydrogen Energy 2008, 33, 6772.
4. Zhanga, Y.; Wanb, Y.; Zhanga, G.; Shaoa, K.; Zhaoa, C.; Li, H.; Naa, H. J Membr Sci 2010, 348, 353.
5. Kumar, S.; Sun, L. L.; Lively, B.; Zhong, W. H. J Nanosci Nanotechnol 2011, 11, 1976.
6. Kumar, S.; Li, B.; Caceres, S.; Maguire, R. G.; Zhong, W. H. Nanotechnology 2009, 20, 465708.
7. Chen, J.; Liu, H.; Weimer, W. A.; Halls, M. D.; Waldeck, D. H.; Walker, G. C. J Am Chem Soc 2002, 124, 9034.
8. Zhang, W. D.; Shen, L.; Phang, I. Y.; Liu, T. Macromolecules 2004, 37, 256.
9. Zhu, J.; Kim, J. D.; Peng, H.; Margrave, J. L.; Khabashesku, V. N.; Barrera, E. V. Nano Lett 2003, 3, 1107.
10. So, H. H.; Cho, J. W.; Sahoo, N. G. Eur Polym J 2007, 43, 3750.
11. Yuen, S. M.; Ma, C. C. M.; Lin, Y. Y.; Kuan, H. C. Comp Sci Technol 2007, 67, 2564.
12. Manea, C.; Mulder, M. J Membr Sci 2002, 206, 443.
13. Kumara, S.; Rath, T.; Mahaling, R. N.; Reddya, C. S.; Dasa, C. K.; Pandey, K. N.; Srivastava, R. B.; Yadaw, S. B. Mater Sci Eng B 2007, 141, 61.
14. Mikhailenko, S. D.; Zaidi, S. M. J.; Kaliaguine, S. Polym Phys 2000, 38, 1386.
15. Kumar, G. G.; Uthirakumar, P.; Nahm, K. S.; Elizabeth, R. N. Solid State Ionics 2009, 180, 282.
16. Neburchilov, V.; Martin, J.; Wang, H.; Zhang, J. J Power Sources 2007, 169, 221.
17. Bijwe, J.; Indumathi, J.; Ghosh, A. K. Wear 2002, 253, 768.
18. Lakshmi, R. T. P. S. M.; Bhattacharya, S.; Varma, I. K. High Performance Polym 2006, 18, 115.
19. Ounaiesa, Z.; Parkb, C.; Wiseb, K. E.; Siochic, E. J.; Harrisonc, J. S. Comp Sci Technol 2003, 63, 1637.
20. Liu, T.; Tong, Y.; Zhang, W. D. Comp Sci Technol 2007, 67, 406.
21. Loredo, D. E. S.; Paredes, M. L. L.; Sena, M. E. Mater Lett 2008, 62, 3319.
22. Pinto, B. P.; Maria, L. C. D. S.; Sena, M. E. Mater Lett 2007, 61, 2540.
23. Shen, L. Q.; Xu, Z. K.; Yang, Q.; Sun, H. L.; Wang, S. Y.; Xu, Y. Y. Inc J Appl Polym Sci 2004, 92, 1709.
24. Rajagopalan, M.; Jeon, J. H.; Oh, I. K. Sensors and Actuators B 2010, 151, 198.
25. Shu, Y. C.; Chuang, F. S.; Tsen, W. C.; Chow, J. D.; Gong, C.; Wen, S. Inc J Appl Polym Sci 2008, 107, 2963.
26. Liu, T.; Tong, Y.; Zhang, W. D. Comp Sci Technol 2007, 67, 406.
27. Yang, T. J Membr Sci 2009, 342, 221.
28. Zhao, X.; Bryan, T.; Chu, T.; Ballesteros, B.; Wang, W.; Jonston, C.; John, M. S.; Patrick, S. G. Nanotechnology 2009, 20, 9.
29. Chen, X.; Chen, X.; Lin, M.; Zhong, W.; Chen, X.; Chen, Z. Macromol Chem Phys 2007, 208, 964.
30. Sadrabadi, M. M. H.; Emamia, S. H.; Moaddel, H. J Power Sources 2008, 183, 551.
31. Woo, Y. T.; Oh, S. Y.; Kanga, Y. S.; Jung, B. J Membr Sci 2003, 220, 31.
32. Soma, G.; Kyonsuku, M. Polymer 2009, 50, 1034.
33. Rajagopalan, M.; Oh, I. K. ACSNANO 2011, 5, 2248.
34. Nagendrana, A.; Vidyaa, S.; Mohana, D. Soft Mater 2008, 6, 45.
35. Goh, P. S.; Ng, B. C.; Ismail, A. F.; Aziz, M.; Sanip, S. M. Solid State Sci 2010, 12, 2155.
36. Pana, H.; Zhua, X.; Chena, J.; Jian, X. J Membr Sci 2009, 326, 453.
37. Guhathakurta, S.; Min, K. J Polym Sci Part B: Polym Phys 2009, 47, 2178.
38. Kobayashi, T.; Rikukawa, M.; Sanui, K.; Ogata, N. Solid State Ionics 1998, 106, 219.
39. Joo, S. H.; Pak, C. H.; Kim, E. A.; Lee, Y. H.; Chang, H.; Seung, D. Y.; Choi, Y. S.; Park, J. B.; Kim, T. K. J Power Sources 2008, 180, 63.
40. Zhou, S.; Wu, Q.; Liu, A. Polym Bull 2006, 56, 95.
41. Mohtar, S. S.; Ismail, A. F.; Matsuura, T. J Membr Sci 2011, 371, 10.
42. Cho, C. G.; Jang, H. Y.; You, Y. G.; Li, G. H.; An, S. G. High Performance Polym 2006, 18, 579.
43. Fu, T.; Cui, Z.; Zhong, S.; Shid, Y.; Zhao, C.; Zhang, G.; Shao, K.; Xing, W. J Power Sources 2008, 185, 32.